Journal of Applied Polymer Science

Influence of Very Long Aging on the Relaxation Behavior of Flame-Retardant Printed Circuit Board Epoxy Composites Under Mechatronic Conditions

Mélanie Lé-Magda,[1,2,3] Eric Dargent,[1] Jorge Arturo Soto Puente,[1] Alain Guillet,[2] Emmanuelle Font,[3] Jean-Marc Saiter[1]

[1]Advanced Materials and Mechanical Engineering-Laboratoire d'Etude et de Caractérisation des Amorphes et de Polymères (AMME-LECAP EA4528) International Laboratory, Université et Institut National des Sciences Appliquées (INSA) de Rouen, avenue de l'Université, 76801 Saint Etienne du Rouvray Cedex, France

[2]Groupe de Physique des Matériaux Unité mixte de recherche (UMR) CNRS Université et Institut National des Sciences Appliquées (INSA) de Rouen, avenue de l'Université, 76801 Saint Etienne du Rouvray Cedex, France

[3]Laboratoire National d'Essai (LNE), 29 avenue Roger Hennequin, 78297 Trappes, France

Correspondence to: E. Dargent (E-mail: eric.dargent@univ-rouen.fr)

ABSTRACT: Very long aging times, up to 15,100 h (629 days) at 110°C, were achieved on flame-retardant printed circuit board laminates commonly used in automotive design. This composite was fabricated from glass fibers embedded in an epoxy resin. Aging was performed in an oven under an air atmosphere at a temperature lower than the glass-transition temperature. Temperature-modulated differential scanning calorimetric analysis was used to investigate the influence of such aging on the glass-transition phenomena. A new amorphous phase appeared during aging. By extending the analysis to samples collected at different thicknesses, we demonstrated the existence of a time-dependent gradient of the properties. A skin–core structure was evidenced, and this slowed down oxidation and allowed physical aging to occur in the bulk sample. An exponential law described the variations of the glass-transition of the new external compound. © 2013 Wiley Periodicals, Inc. J. Appl. Polym. Sci. 130: 786–792, 2013

KEYWORDS: aging; composites; differential scanning calorimetry (DSC); glass transition; thermosets

Received 26 September 2012; accepted 18 February 2013; published online 4 April 2013
DOI: 10.1002/app.39216

INTRODUCTION

Epoxy resins are widely used in advanced composites to provide dimensional stability, elevated mechanical performance, and good chemical, electrical, and thermal resistances.[1,2] In automotive design, flame-retardant printed circuit board (PCB FR4) is the most commonly used grade for glass epoxy laminates. It is fabricated from woven glass fiber incorporated into an epoxy resin, in which a flame retardant is added for safety purposes.[3] The National Electrical Manufacturers Association regulates the different standards. One of them, the FR-4 standard, typically employs bromide (a halogen) to facilitate flame-resistant properties. For these mechatronic systems, the requirements are stringent and impose no chemical or mechanical modifications after 1000 h at 110°C. Several tests (mainly tensile tests performed at cryogenic temperatures) have been done on these systems in the military[4] and aeronautic[5] fields; however, no investigations have been carried out for very long aging times (t_a's). Aging is commonly understood as a change in the material properties with time, and it is of prime importance to know or at least to predict what a device's evolution will be during its lifespan. Hence, the objective of several studies performed in different laboratories has been the development of protocols to simulate and/or accelerate the effects of aging. Generally, the aging of a thermoset resin such as epoxy resin can be explored with two separate and complementary routes, which are typically defined as physical and chemical aging.[1,6–8]

With regard to the latter, we may, for instance, distinguish between the respective influence of molecules such as O_2, H_2O, or solvents and the absorption of light (mainly UV) on the material's aging evolution. Most of the time, the chemical bonds (covalent, hydrogen, van der Waals) cause irreversible modification. For epoxy-based resins, some studies have been concerned with hygrothermal aging.[9–11] It has been shown that in addition to the well-known plasticization effect due to water molecule absorption, modifications of the crosslinking density occur and drastically change the mechanical performance.[12] The thermal

oxidation of epoxy–amine networks exposed to air between 140 and 195°C revealed that the oxidized layer profile was hyperbolic.[13] Thus, depending on the t_a, it is expected that oxidation will lead to a gradient of properties in the thickness of the device. The addition of bromide as a flame retardant to an epoxy resin destabilizes the thermoset system, which becomes less stable than nonbrominated ones.[14]

The second aspect of aging is linked to the disordered structure of the thermoset resin. From a physical point of view, the structure is a glass; this implies the existence of a glass transition [characterized by the glass-transition temperature (T_g)]. If aging is performed at temperatures below T_g, the well-known physical aging, also called *structural relaxation*,[15] occurs. Compared with the thermodynamic equilibrium state, the glassy state of an amorphous polymer is characterized by an excess of free volume, an excess of enthalpy, and an excess of entropy. This explains why all of the physical properties of a thermosetting resin are time dependent. Investigations concerning physical aging in epoxy systems are numerous,[16–18] and different techniques have been used, including positron annihilation lifetime spectroscopy and differential scanning calorimetry (DSC).[19,20] A review of the current understanding of physical aging in various epoxy polymers and in epoxy-based composites was done by Odegard and Bandyopadhyay.[21] For technical reasons, in different articles already published, the t_a was limited to some thousand hours. For example, both the hydrothermal and physical aging of epoxy–amine (diglycidyl ether of Bisphenol A–4,4′-methylene bis[3-chloro-2,6-diethylaniline] (DGEBA–MCDEA) networks[22] showed that the physical aging was affected by hydrothermal action after 2000 h of aging. When only one parameter (e.g., the temperature) was varied, the duration of the test fell down to between 120 and 4000 h (120,[19] 168,[23] 350,[24] 361,[25] 500,[26] 1000,[5] 2880,[27] and 4000 h[8]). Physical aging has often been investigated with standard DSC[16,18,25,28] and aging performed *in situ*[23,29] or in an oven.[19,30]

For a printed circuit boards based on tetrabromobisphenol A–diglycidyl ether (PCB FR4), the automotive industry requires that their life duration must be at least 10 years. It is clear that until now, it has been very difficult to propose a statistical model to predict such long-term behavior because of the complexity of the constraints (e.g., temperature, humidity, vibrations) to which the final device is exposed. One possible way to do this is to perform experiments at the highest possible temperature but below T_g and to drastically increase the experimental time of aging. Therefore, in this study, we investigated the influence of very long aging times at 110°C (the T_g was expected to be 130°C), for up to 15,100 h (21 months) under an air atmosphere. Previous studies have clearly identified a time-dependent oxidation process for PCB FR4 and equivalent epoxy-based devices. Pei et al.[27] showed by dynamic mechanical thermal analysis that thermal oxidative aging at T_a higher than T_g led to the appearance of a new compound, and two glass transition were evidenced, although aging at $T_a < T_g$ (110°C) did not allow the detection of an extra amorphous phase ($t_a \leq$ 2880 h). In a recent study,[31] we showed by Fourier transform infrared spectroscopic analysis that PCB FR4 aged at 110°C under an air atmosphere initiated the oxidation process and could produce ketones, acids, or other oxygenated products and, consequently, changed the chemical structure of the material, even for very small t_a's (940 h). As the chemical structural changes during aging, the kinetics of the physical aging must also be affected, and this is probably dependent on the magnitude of the oxidation undergone by PCB FR4.

In this study, we focused on the consequence of chemical aging on the physical aging processes occurring in PCB FR4. Mainly, the DSC and temperature-modulated differential scanning calorimetry (TMDSC) analytical techniques were used. Because an oxidative process existed, the study was performed with samples collected at different depths from the surface of the PCB FR4. This allowed us to track the process as a function of the depth from the surface.

EXPERIMENTAL

The composite, PCB FR4 KB6160, was provided by the Chinese company King Board (Shaoguan, China) as a panel of circuit printed board 60 × 40 cm^2 in dimension. The specimens were sampled from this panel, and all copper coatings were removed before testing. The material composition, determined previously by thermogravimetry,[31] was 52 wt % glass fiber and 48 wt % epoxy resin. The aging was performed in a Memmert oven at 110°C under an air atmosphere for t_a's between 0 and 15 × 10^3 h. The initial T_g (midpoint T_g on the DSC curve) measured in this study was 128°C. Consequently, physical aging was performed at T_a = 110°C = T_g − 18°C. Samples having an average thickness of 1.6 mm were cut at midthickness and cut again to obtain three slides that represented three different depths in the sample. The external part (100–300 μm), intermediate part (300–600 μm), and internal part (600–800 μm) were obtained.

DSC and TMDSC were performed on a TA Instruments (New Castle, DE, USA) apparatus (DSC 2920). The temperature and energy calibrations were carried out with standard values of indium and zinc. The specific heat capacities for each sample with different t_a's were measured with sapphire as a reference. The sample masses were close to that of the reference, that is, approximately 20 mg. After the first run (DSC), the samples were cooled at 20°C/min, and a second run (TMDSC) was immediately performed. The TMDSC experiments were performed with an oscillation amplitude of ±1°C, an oscillation period of 100 s, and a heating rate of 3°C/min. All of these measurements were carried out under a nitrogen atmosphere. Because the glass fibers did not give any signal on the DSC curve, the signal was normalized to the actual content of epoxy. From TMDSC, different signals could be obtained: the heat flow and the apparent complex heat capacity (C_p^*).[32] From the ratio between the amplitude of the modulated heat flow (A_q) and the amplitude of the heating rate (A_β), it was possible to extract C_p^* according to eq. (1):

$$|Cp^*| = \frac{A_q}{A_\beta} \times \frac{1}{m} \quad (1)$$

where m is the polymer mass. Because of the phase lag (ϕ) between the calorimeter response function (i.e., the heat flow)

Applied Polymer SCIENCE

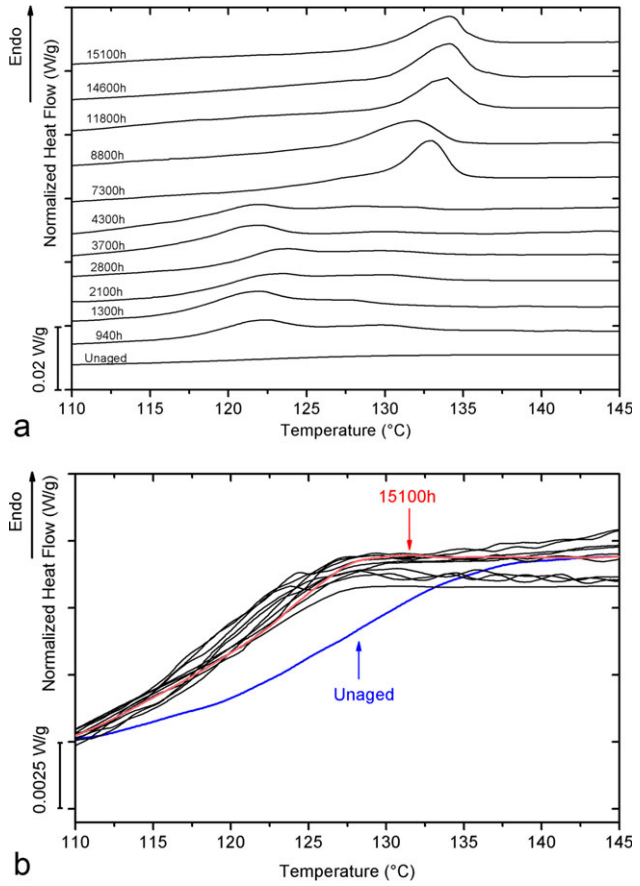

Figure 1. Normalized heat flow curves of the unaged and differently aged samples of PCB FR4: (a) first run: DSC (heating rate = 3°C/min) and (b) second run: TMDSC (heating rate = 3°C/min, period = 100 s, and amplitude = ±1°C). [Color figure can be viewed in the online issue, which is available at wileyonlinelibrary.com.]

and the time derivative of the modulated temperature program, two components [the in-phase and out-of-phase components of the apparent complex heat capacity (C' and C'', respectively)] could be calculated according to the following equations:

$$C' = \left|C_p^*\right| \cos \phi \tag{2}$$

$$C'' = \left|C_p^*\right| \sin \phi \tag{3}$$

In this study, C' and C'' were systematically analyzed. The C' versus temperature variations usually appeared as an endothermic step, and the C'' variations showed a peak in the T_g region. More details concerning the determination of C_p^*, especially the correction of the measured phase angle for contributions originating from heat transfer, were given by Weyer et al.[33]

RESULTS

Figure 1(a) shows the DSC curves of samples aged up to 15 × 10^3 h. For all of the aged samples, complex endothermic signals were superimposed onto the endothermic step characteristics of the glass transition. Depending on the t_a of the sample, it appeared that up to 4300 h, the signal at T_g showed two more or less observable endothermic peaks, one with a relative large magnitude in the temperature range 115–125°C and another with a low magnitude between 125 and 135°C. For t_a's higher than 7300 h, a single endothermic peak appeared between 127 and 137°C. After each heating step, the sample was cooled down to room temperature at 20°C/min and was finally heated again to analyze the possibility of rejuvenation. Figure 1(b) shows the TMDSC curves obtained during these second runs. For all of the samples, the endothermic step was observed between 115 and 145°C, and it was different for the unaged and the aged samples. Figure 2(a,b) shows enlargements of Figure 1 but only for the unaged sample and for samples aged at 2100 and 15 × 10^3 h. Figure 2(a) shows the DSC thermogram of the samples, whereas Figure 2(b) displays the TMDSC analysis of the same specimens during the second heating and, therefore, without physical aging. These figures confirmed the complexity of the signal occurring at T_g. The heat capacity step [$\Delta C_p(T_g)$] was determined by $C_{pl} - C_{pg}$ at T_g, where C_{pl} is the value of the heat capacity extrapolated from the liquidlike or rubbery state temperature domain to T_g and C_{pg} is the heat capacity extrapolated from the glassy temperature domain up to T_g. We noted a significant difference in $\Delta C_p(T_g)$ between the virgin and the aged samples. However, this difference vanished when the second heating was applied to the samples. Because flame

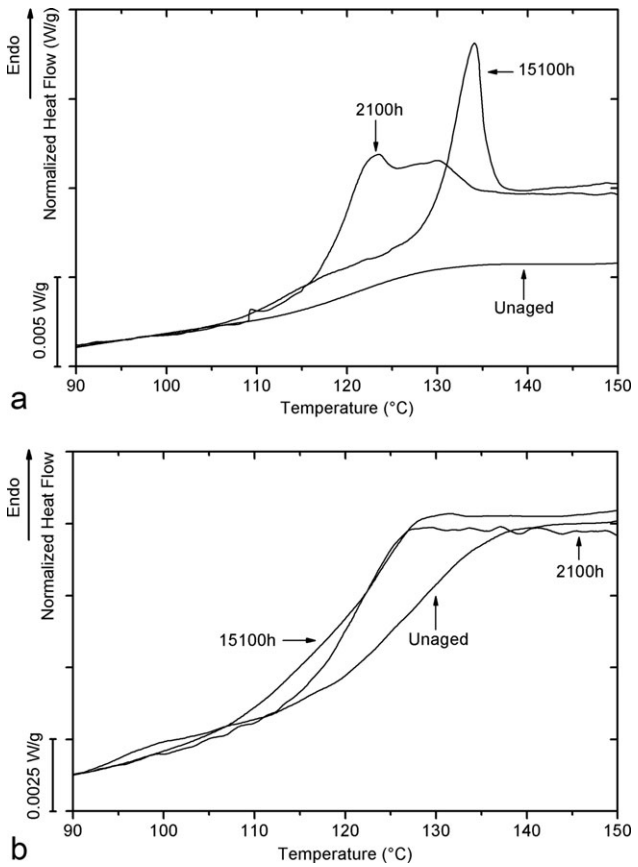

Figure 2. DSC thermograms of the unaged and aged (2100 and 15,100 h) PCB FR4: (a) first run: DSC (heating rate = 3°C/min) and (b) second run: TMDSC (heating rate = 3°C/min, period = 100 s, and amplitude ±1°C).

Table I. DSC and TMDSC Results

t_a (h)	δH (J/g; DSC HF)	T_g (°C; TMDSC C′)	$T_{\alpha 1}$ (°C; TMDSC C″)	$T_{\alpha 2}$ (°C; TMDSC C″)
0	0	130	129	—
940	0.31	125	122	—
1,300	0.62	122	122	—
2,100	0.57	121	122	114
2,800	0.58	121	123	114
3,700	0.46	120	123	114
4,300	0.53	120	124	114
7,300	0.80	124	124	114
8,800	1.55	124	126	115
11,800	1.63	123	126	114
14,600	1.88	123	127	115
15,100	1.70	124	127	115

δH, enthalpy associated with the relaxation peak observed during the first DSC Heat Flow run; T_g, glass-transition midpoint temperature determined from the C′ signal; T_α, maximum of the C″ peaks.

retardants were present in the unaged sample during the first heating, they may have influenced the specimen response. When we subtracted the curve of the second run from that of the first run, the curve obtained, once integrated, allowed the calculation of the recovery enthalpy (δH); this corresponded to the energy needed for the sample to again reach equilibrium (liquidlike or rubbery state) at a temperature greater than T_g. δH is reported in Table I as a function of the t_a of the sample.

The TMDSC C_p^* curves are reported in Figure 3 for C'' observed on three samples with different aging histories. The C' signals are not shown here but were present at ΔC_p at T_g; this allowed the precise determination of T_g (Table I). Figure 3 shows the C'' signals of the unaged sample and the aged samples with $t_a >$ 1300 h and $t_a >$ 4300 h. Because the C'' signal was obtained from the reversing heat flow, the enthalpic contribution characteristic of physical aging (i.e., the endothermic peak) was not observed. The C'' signals were indicative of the distribution of the molecular mobility at the glass transition.[34] The C'' peaks for $t_a >$ 4300 h was clearly bimodal; this was indicative of the existence of two glass transitions. The temperature at the maximum (T_α) characterized the α transition, which corresponded to the so-called dynamic glass transition. The extra peak, which appeared at a lower temperature, was defined as peak 2 ($T_{\alpha 1}$), and the upper peak was defined as peak 1 ($T_{\alpha 2}$). The values of $T_{\alpha 1}$ and $T_{\alpha 2}$ after mathematical treatment are reported in Table I (see Discussion section). A direct analysis of the TMDSC C'' signals confirmed the DSC observations that indicated that two amorphous phases existed.

DISCUSSION

First, we assumed that the parameters characteristic of physical aging were representative of the total volume of the sample analyzed. This assumption means that the effects of the chemistry and mainly oxidation concerned the entire sample. T_g decreased from 130 to 120°C at the beginning of the aging period, and then a threshold was observed: T_g jumped to reach a quasi-constant value close to 124°C (Figure 4). These variations of T_g with time could not be explained by a standard physical aging process because physical aging is known to continuously increase the value of T_g to a constant value, where equilibrium is reached.[23,25] These variations of T_g with time could also not be explained by the existence of a postcuring reaction associated with the thermal cycles performed during the study because it is known that a postcuring reaction leads to a continuous increase in the value of T_g.[35] For these materials, it was demonstrated that an oxidation process occurred[31] and led to chain scissions, which resulted in more molecular mobility. Thus, during this first stage of aging, the molecular mobility increased, and consequently, T_g decreased. For $t_a >$ 4300 h, T_g was constant. This indicated that the oxidation process was no longer possible. The evolution of δH as a function of the aging duration is also reported in Figure 4. The expected sigmoidal curve characteristic of physical aging[36] and indicative of a nonlinear and nonexponential behavior was not observed; this was the case for

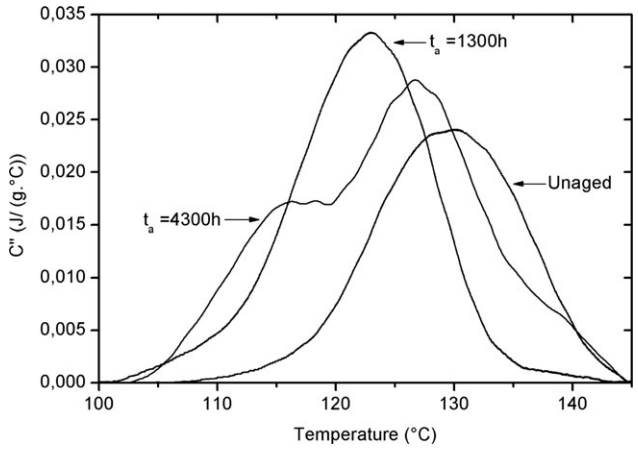

Figure 3. Typical C″ curves for three aged samples: unaged, short t_a, (t_a = 1300 h), and long t_a (t_a = 4300 h).

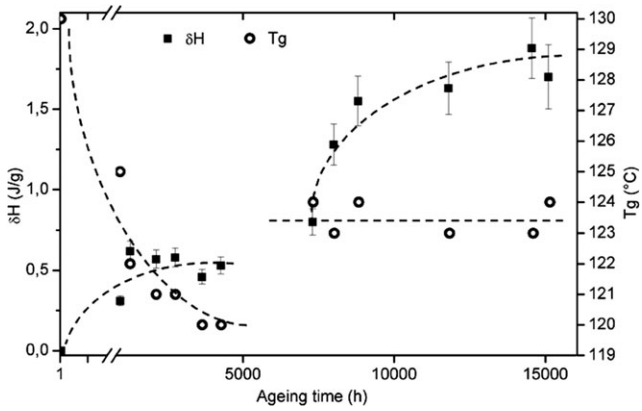

Figure 4. Evolution of δH and T_g with t_a. The T_g values were obtained by TMDSC analysis from the C′ signals.

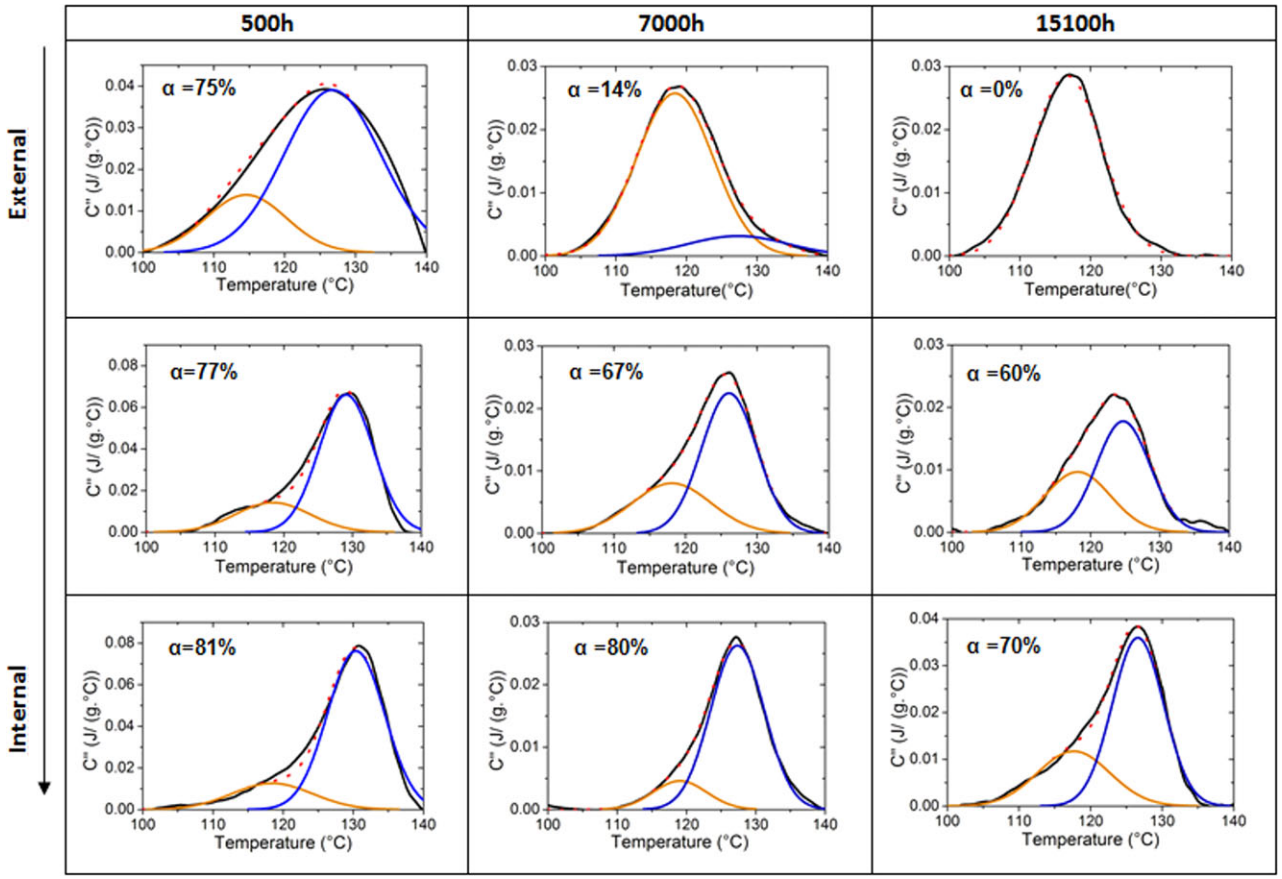

Figure 5. C″ curves from TMDSC analysis for three aged samples (500, 7,000, and 15,100 h) at different depths. The new compound fraction (α) is shown as an insert. Samples having an average thickness of 1.6 mm were cut at midthickness and cut again to obtain three slides that represented three different depths in the sample. External part (100–300 μm), intermediate part (300–600 μm), and internal part (600–800 μm). [Color figure can be viewed in the online issue, which is available at wileyonlinelibrary.com.]

Bandyopadhyay and Odegard[37] (δH was found to vary quasi-linearly with ln t_a for four sets of data obtained on an equivalent system aged at $T_a = T_g - 40°C$). For a homogeneous glassy medium, δH expected after an infinite duration is given by $\delta H_\infty = \Delta C_p(T_g - T_a)$. It followed that the expected δH at equilibrium for our system could have been $\delta H_\infty = 7.2$ J/g. After aging for 15×10^3 h, a value of $\delta H = 1.7$ J/g was obtained; this indicated that the material was still far away from equilibrium.

This former analysis, which assumed the existence of a homogeneous glassy material, could not be maintained to quantify the phenomenon involved during aging. For instance, the quantitative role of oxidation from the interface initially omitted had to be included in the discussion, and finally, the existence of two signals at the glass transition had to be taken into account. The existence of two signals at the glass transition was reported by Polansky et al.[26] and Pei et al.[27] with DSC or dynamical mechanical analysis (DMA) methods and aging temperatures above T_g. They proposed the existence of two amorphous phases (one occurring as the result of aging). Our aging experiments were performed below T_g; this meant a domain of temperature for which the molecular mobility of the chains or chain segments was drastically reduced. Taking into account our previous results[31] showing the existence of a thermal oxidative process, it follows that aging below T_g led to thermal degradation, which did not necessarily concern the entire volume of the sample. The difference between the values of $T_{\alpha 1}$ and $T_{\alpha 2}$ reflected the degree of oxidative degradation. With regards to the data obtained, we proposed a fit of the time dependence of $\Delta T_g = T_{\alpha 2} - T_{\alpha 1}$ by means of an exponential law according to

$$\Delta T_g = T_{\alpha 2} - T_{\alpha 1} = A \exp(-Kt_a) + \Delta T_{g^\infty} \quad (4)$$

where A and K are material constants and $\Delta T_{g\infty}$ is the value of $T_{\alpha 2} - T_{\alpha 1}$ when t_a reaches infinity. By fitting the data with eq. (4), we found values of $K = 0.003$ days^{-1}, $A = 4.5$ K, and $\Delta T_{g\infty} = -12$ K. An equivalent relationship was used by Pei et al.[27] to describe the effects of oxidative aging on epoxy samples performed at temperatures above T_g. The following set of data was obtained for $T_a = 150°C$: $K = 0.03$ days^{-1}, $A = -78$ K, $\Delta T_{g\infty} = 71$ K. It is not surprising that the values of A, K, and $\Delta T_{g\infty}$ were different between the two experiments because the materials were not in the same state (above and below T_g). We found that the kinetic parameter K of the process was 10 times lower for the glassy material than for the caoutchoutic one (i.e., $T > T_g$).

Polansky et al.[26] showed the degradation of particular small regions in aged PCB FR4. The possibility of a gradient of the

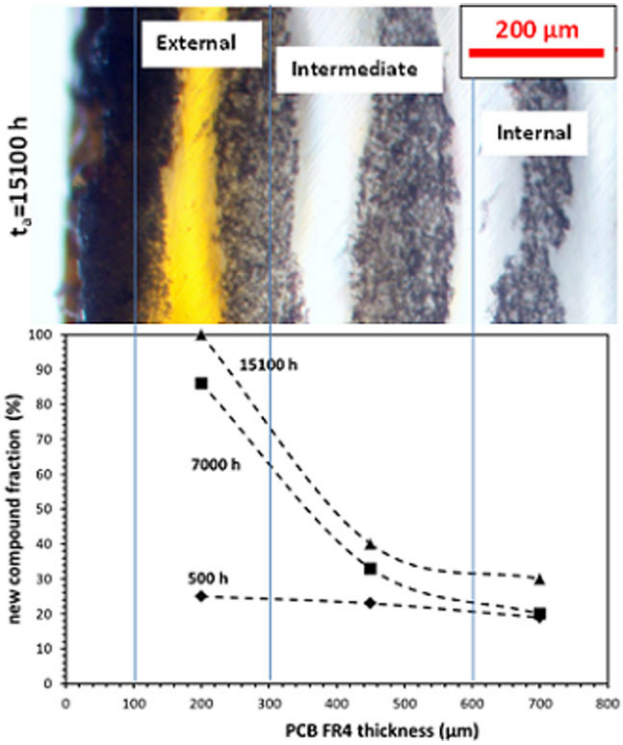

Figure 6. New compound fraction (α) as a function of the thickness. Samples having an average thickness of 1.6 mm were cut at midthickness and cut again to obtain three slides that represented three different depths in the sample. External part (100–300 μm), intermediate part (300–600 μm), and internal part (600–800 μm). Optical microscopy showed organic layers separated by glass fibers for the t_a = 15,100 h sample. The scale is the same for the graph and the picture. [Color figure can be viewed in the online issue, which is available at wileyonlinelibrary.com.]

degraded structure within the thickness of PCB FR4 sample had to be considered. To do this, TMDSC analysis was carried out on samples extracted at different depths and for different t_a's. The C'' curves obtained are reported in Figure 5. For the same aging duration, it was clear that the signal was not the same when the samples were on the surface or in the middle of the PCB FR4 specimen. A gradient of the properties was demonstrated. Differences as a function of the depth for the signal for the short t_a (500 h) were clear. The C'' signal exhibited two contributions: one with a small magnitude at low temperature and one with a large magnitude at high temperature. It was possible to isolate each contribution by a fitting procedure under the assumption that each contribution was described by a Gaussian statistical function. The Gaussian curves are also displayed in Figure 5 and are superimposed onto each initial signal. Using this fitting procedure for each signal, we observed that the magnitude of the low-temperature contribution increased with time, whereas the high-temperature contribution totally disappeared for samples taken at the surface of PCB FR4 for long degradation times. From the integration of each peak, the percentage of the new compound (α; the peak at low temperature) on the whole organic fraction of PCB FR4 was calculated (reported in Figure 5). The variations of α as a function of the thickness are reported in Figure 6 for the three t_a's, and the optical microscopy pictures obtained at t_a = 15,100 h are also shown. One can see a very dark skin at the surface (100–300 μm, TMDSC external part). The organic layer between the glass fibers was yellow. Observable changes in color are known to be indicative of thermooxidative degradation.[21] For the intermediate and internal parts, the organic layer remained white, as for the unaged samples. The images confirmed that degradation took place in the external part, and a skin–core structure was evident. The skin represented approximately 38% of the volume of PCB FR4. The chemical degradation was highly active at the surface up to durations of 7000 h [this corresponded to the threshold observed in Figure 4 and the change in the DSC curves in Figure 1(a)]. On the other hand, the increase in α was very low with t_a for the internal and the intermediate zones. The new chemically modified layer appearing at the surface probably created a barrier effect that blocked the oxidation process at greater depths of the PCB FR4 device because α increased in the internal zone from only 20 to 30% between 7000 and 15,100 h. Then, physical aging could have played a role in the lifetime of the PCB FR4 device, as shown in Figure 4.

CONCLUSIONS

During aging of PCB FR4 at T_a's lower than T_g (T_a = 110°C), thermal oxidative reactions began at the surface and progressed through the sample thickness. A new amorphous phase appeared for t_a's as low as 500 h at the surface. The difference between the T_g's followed an exponential law of small amplitude. The new phase progressively blocked the diffusion of dioxygen, and a skin–core microstructure occurred for times higher than 7000 h. Hence, between 0 and 7000 h, aging was governed by chemical modification, whereas for aging times longer than 7000 h, the rate of chemical modification decreased drastically. Because few chemical reactions occurred, physical aging could take place progressively. After a long aging of 15,100 h, the material was still far from being at equilibrium. Finally, TMDSC was shown to be a powerful tool for obtaining quantitative information on the polymeric fraction of the composite at each of the t_a's.

ACKNOWLEDGMENTS

The authors thank Peter Mallon of Stellenbosch University (South Africa) for fruitful discussions.

REFERENCES

1. De Fenzo, A.; Formicola, C.; Antonucci, V.; Zarrelli, M.; Giordano, M. *Polym. Degrad. Stab.* **2009**, *94*, 1354.
2. Wang, D. Z. Production and Application of Epoxy Resin; Chemical Industry Press: Beijing, **2001**.
3. Permadi; Castro, J. M. *J. Appl. Polym. Sci.* **2004**, *91*, 1136.
4. Yuan, F.; Tsai, L.; Prakash, V.; Rajendran, A. M.; Dandekar, D. P. *Int. J. Solids Struct.* **2007**, *44*, 7731,
5. Dao, B.; Hodgkin, J.; Krstina, J.; Mardel, J.; Tian, W. *J. Appl. Polym. Sci.* **2006**, *102*, 4291.

6. Kong, E. S. W.; Wilkes, G. L.; McGrath, J. E.; Banthia, A. K.; Mohajer, Y.; Tant, M. R. *Polym. Eng. Sci.* **1981**, *21*, 943.
7. Le Huy, H. M.; Bellenger, V.; Verdu, J.; Paris, M. *Polym. Degrad. Stab.* **1992**, *35*, 77.
8. Ciutacu, S.; Budrugeac, P.; Niculae, I. *Polym. Degrad. Stab.* **1991**, *31*, 365.
9. Lin, Y. C.; Chen, X. *Polymer* **2005**, *46*, 11994.
10. Bockenheimer, C.; Fata, D.; Possart, W. *J. Appl. Polym. Sci.* **2004**, *91*, 369.
11. Zhou, J.; Lucas, J. P. *Polymer* **1999**, *40*, 5513.
12. Alessi, S.; Conduruta, D.; Pitarresi, G.; Dispenza, C.; Spadaro, G. *Polym. Degrad. Stab.* **2011**, *96*, 642.
13. Damian, C.; Espuche, E.; Escoubes, M. *Polym. Degrad. Stab.* **2001**, *72*, 447.
14. Balabanovich, A. I.; Hornung, A.; Merz, D.; Seifert, H. *Polym. Degrad. Stab.* **2004**, *85*, 713.
15. Struik, L. C. E. Physical Aging in Amorphous Polymers and Other Materials; Elsevier: Amsterdam, **1978**.
16. Calventus, Y.; Montserrat, S.; Hutchinson, J. M. *Polymer* **2001**, *42*, 7081.
17. Ramirez, C.; Abad, M. J.; Cano, J.; Lopez, J.; Nogueira, P.; Barral, L. *Colloid Polym. Sci.* **2001**, *279*, 184.
18. Montserrat, S.; Ribelles, J. L. G.; Meseguer, J. M. *Polymer* **1998**, *39*, 3801.
19. Wang, B.; Gong, W.; Liu, W. H.; Wang, Z. F.; Qi, N.; Li, X. W.; Liu, M. J.; Li, S. J. *Polymer* **2003**, *44*, 4047.
20. Bockenheimer, C.; Fata, D.; Possart, W. *J. Appl. Polym. Sci.* **2004**, *91*, 361.
21. Odegard, G. M.; Bandyopadhyay, A. *J. Polym. Sci. Part B: Polym. Phys.* **2011**, *49*, 1695.
22. Colombini, D.; Martinez-Vega, J. J.; Merle, G. *Polymer* **2002**, *43*, 4479.
23. Barral, L.; Cano, J.; Lopez, J.; Lopez-Bueno, I.; Nogueira, P.; Abad, M. J.; Ramirez, C. *Eur. Polym. J.* **1999**, *35*, 403.
24. Chen, X.; Li, S. *Polym. Eng. Sci.* **1998**, *38*, 947.
25. Fraga, F.; Castro-Díaz, C.; Rodríguez-Núñez, E.; Martínez-Ageitos, J. M. *Polymer* **2003**, *44*, 5779.
26. Polansky, R.; Mentlık, V.; Prosr, P.; Susır J. *Polym. Test.* **2009**, *28*, 428.
27. Pei, Y. M.; Wang, K.; Zhan, M. S.; Xu, W.; Ding, X. *J. Polym. Degrad. Stab.* **2011**, *96*, 1179.
28. Ornaghi, H. L., Jr.; Pistor, V.; Zattera, A. J. *J. Non-Cryst. Solids* **2012**, *358*, 427.
29. Ramirez, C.; Abad, M. J.; Cano, J.; Lopez, J.; Nogueira, P.; Barral, L. *Colloid Polym. Sci.* **2001**, *279*, 184.
30. Jo, W. H.; Ko, K. *J. Polym. Eng. Sci.* **1997**, *31*, 239.
31. Lé-Magda, M.; Dargent, E.; Youssef, B.; Guillet, A.; Idrac, J.; Saiter, J. M. *Macromol. Symp.* **2012**, *315*, 143.
32. Delpouve, N.; Saiter, A.; Mano, J.; Dargent, E. *Polymer* **2008**, *49*, 3130.
33. Weyer, S.; Hensel, A.; Schick, C. *Thermochim. Acta* **1997**, *304–305*, 267.
34. Saiter, A.; Delpouve, N.; Dargent, E.; Saiter, J. M. *Eur. Polym. J.* **2007**, *43*, 4675.
35. Delahaye, N.; Marais, S.; Saiter, J. M.; Metayer, M. *J. Appl. Polym. Sci.* **1998**, *67*, 695.
36. Lixon-Buquet, C.; Hamonic, F.; Saiter, A.; Dargent, E.; Langevin, D.; Nguyen, Q. T. *Thermochim. Acta* **2010**, *509*, 18.
37. Bandyopadhyay, A.; Odegard, G. M. *J. Appl. Polym. Sci.* **2013**, *128*, 660.